

**INVESTIGATION ON CANCER  
CHEMOPREVENTIVE ACTIVITY OF  
FABRICATED TQ ENCAPSULATED PLGA-PF68  
NANOPARTICLES ON SELECTED BREAST  
CANCER CELL LINES**

**NURUL SHAHFIZA BINTI NOOR**

**UNIVERSITI SAINS MALAYSIA**

**2022**

**INVESTIGATION ON CANCER  
CHEMOPREVENTIVE ACTIVITY OF  
FABRICATED TQ ENCAPSULATED PLGA-PF68  
NANOPARTICLES ON SELECTED BREAST  
CANCER CELL LINES**

by

**NURUL SHAHFIZA BINTI NOOR**

**Thesis submitted in fulfilment of the requirements  
for the degree of  
Doctor of Philosophy**

**February 2022**

## ACKNOWLEDGEMENT

First and foremost, thank you Allah, the Almighty for giving me the opportunity to embark on my PhD and for completing this long and challenging journey successfully.

My sincere gratitude to my supervisor, Associate Professor Dr. Shahrul Bariyah Sahul Hamid for her guidance throughout this research. I would not have been able to complete this journey without her continuous support, encouragement, and patience. I would also like to thank you Dr. Noor Haida Mohd Kaus for her help and encouragement. I extend my appreciation to Prof. Szewczuk and Dr. Gokula Kumar Appalanaido. I also would like to thank the statistician, Mr. Nizuwan Azman for his advice in statistical analysis.

My appreciation goes to my colleagues and friends for helping me with this project. It was indeed a great experience working together in the laboratory. Not to forget, to all staffs including in AMDI, School of Chemical Sciences, and Malaysian Institute of Pharmaceuticals and Nutraceuticals (Ipharm) for the help and support with equipment handling.

Most importantly, this thesis is dedicated to my family for their unwavering love and encouragement throughout this PhD process. This piece of victory is specially dedicated to my mum for her dua', unconditional love and waiting patiently for me to finish this PhD journey. Alhamdulillah.

Last but not least, I want to thankful to the sponsors, Ministry of Higher Education Malaysia and Universiti Sains Malaysia for the precious study opportunity and financial support.

## TABLE OF CONTENTS

<b>ACKNOWLEDGEMENT</b> .....	<b>ii</b>
<b>TABLE OF CONTENTS</b> .....	<b>iii</b>
<b>LIST OF TABLES</b> .....	<b>viii</b>
<b>LIST OF FIGURES</b> .....	<b>xi</b>
<b>LIST OF SYMBOLS</b> .....	<b>xix</b>
<b>LIST OF ABBREVIATIONS</b> .....	<b>xx</b>
<b>LIST OF APPENDICES</b> .....	<b>xxii</b>
<b>ABSTRAK</b> .....	<b>xxiii</b>
<b>ABSTRACT</b> .....	<b>xxv</b>
<b>CHAPTER 1 INTRODUCTION</b> .....	<b>1</b>
1.1 Breast Cancer: An Overview.....	1
1.2 Breast Cancer Treatment .....	4
1.3 Tamoxifen .....	6
1.3.1 Tamoxifen Metabolism .....	7
1.4 Chemoresistance.....	10
1.5 <i>Nigella sativa</i> .....	13
1.6 Thymoquinone: A Promising Drug for Circumventing Multidrug Resistance (MDR) .....	14
1.7 Nanoparticulates to Treat Breast Cancer .....	19
1.7.1 Liposomes .....	25
1.7.2 Nab Paclitaxel .....	26
1.7.3 Polymeric Nanoparticles .....	26
1.8 Co-Polymers and Surfactant.....	28
1.9 Nanomedicines and Clinical Advances of Plant-Derived Compounds in Breast Cancer.....	31
1.9.1 Paclitaxel Nanoparticles .....	32

1.9.2	Camptothecin Nanoparticles .....	32
1.9.3	Curcumin Nanoparticles.....	35
1.9.4	Thymoquinone Nanoparticles .....	36
1.10	NF- $\kappa$ B, an active player of human breast cancer .....	39
1.11	TQ Role in Inhibiting NF- $\kappa$ B.....	41
1.12	Problem Statement .....	41
1.13	Hypothesis.....	44
1.14	Rationale of the Study .....	44
1.15	Objective of Study.....	45
<b>CHAPTER 2</b>	<b>MATERIALS AND METHODOLOGY.....</b>	<b>47</b>
2.1	Materials.....	47
2.2	Methods.....	52
2.2.1	Cell Culture and Culture Conditions.....	52
2.2.2	Generation of Drug Resistant Cell Line.....	52
2.2.3	Confirmation of Drug Resistant Cell Line.....	55
2.2.3(a)	Cell Viability assay.....	55
2.2.3(b)	P-gp Expression Detection using Flow Cytometry Method.....	57
2.2.3(c)	Analysis of Morphological Changes .....	58
2.2.4	Development of Thymoquinone-Nanoparticles (TQ-Np) by Emulsification-Solvent Evaporation Technique .....	58
2.2.5	Physico-Chemical Characterisation of TQ-PLGA-PF68 Nanoparticles.....	60
2.2.5(a)	Functional Groups Quantitation of TQ-PLGA-PF68 Nanoparticles by using FT-NIR Spectroscopic Analysis .....	60
2.2.5(b)	Measurement of Particle Size, Polydispersity Index (PdI) and Zeta Potential (ZP) of TQ-PLGA-PF68 Nanoparticles .....	61
2.2.5(c)	Morphology of TQ-PLGA-PF68 Nanoparticles.....	63

2.2.5(d)	Encapsulation Efficiency (EE) of TQ-PLGA-PF68 Nanoparticles .....	63
2.2.5(e)	Drug Release Profile of TQ-PLGA-PF68 Nanoparticles .....	64
2.2.6	Biological Evaluation of TQ-PLGA-PF68 Nanoparticles .....	66
2.2.6(a)	Cell Viability Assay.....	66
2.2.6(b)	Colony Forming Assay .....	67
2.2.6(c)	Wound Healing Assay .....	68
2.2.6(d)	Rhodamine 123 (Rh123) Efflux Assay.....	69
2.2.6(e)	P-gp Cell Surface Expression .....	70
2.2.7	Analysis of Apoptosis with Terminal Deoxynucleotidyl Transferase-Mediated dUTP Nick-End Labelling (TUNEL) Assay .....	71
2.2.7(a)	TUNEL assay procedure for Flow Cytometry Technique .....	71
2.2.7(b)	TUNEL Assay Procedure for Fluorescence Microscopy Technique .....	74
2.2.8	Observation of TQ-PLGA-PF68 Nanoparticles Internalisation in TamR MCF 7 cells .....	77
2.2.9	Relative Gene Expression Analysis .....	79
2.2.9(a)	Total RNA Extraction and Purification using RNeasy Plus Mini Kit.....	80
2.2.9(b)	cDNA Synthesis using RT <sup>2</sup> First Strand Kit.....	82
2.2.9(c)	Real-time PCR using RT <sup>2</sup> Profiler PCR Array System and RT <sup>2</sup> SYBR® Green Mastermix.....	83
2.2.10	Determination of Signaling Pathway by Gene Annotation.....	87
2.2.11	Proteomic Analysis .....	87
2.2.11(a)	Western Blot Analysis on MDR1/P-gp and NF-κB Protein Expression .....	88
2.2.11(b)	Flow Cytometry Analysis of p21 Waf1/Cip1 Protein Expression.....	94
2.2.12	Statistical Analysis .....	95

<b>CHAPTER 3</b>	<b>DEVELOPMENT OF DRUG RESISTANT BREAST CANCER CELL MODELS .....</b>	<b>96</b>
3.1	Results .....	96
3.1.1	Generation of Tamoxifen and Paclitaxel-Resistant in MCF 7, UACC 732 and MDA-MB 231 cell lines.....	96
3.1.2	Titration of Drug Sensitivity in Drug-Resistant Cell Lines .....	101
3.1.3	P-gp Cell Surface Expression in Drug-Resistant Cell Lines.....	102
3.1.4	P-gp Efflux Activity in Drug-Resistant Cell Lines .....	106
3.1.5	Morphological Features in Drug-Resistant Cell Lines.....	109
3.2	Discussion .....	113
3.3	Conclusion.....	118
<b>CHAPTER 4</b>	<b>DEVELOPMENT OF TQ-PLGA-PF68 NANOPARTICLES.....</b>	<b>119</b>
4.1	Results .....	119
4.1.1	Physico-Chemical Characterisation of TQ-PLGA-PF68 Nanoparticles.....	119
4.1.1(a)	FTIR Spectroscopic Study.....	119
4.1.1(b)	Particle Size, Polydispersity Index (PdI) and Zeta Potential (ZP) Stability of TQ-PLGA-PF68 Nanoparticles .....	122
4.1.1(c)	Morphology of TQ-PLGA-PF68 Nanoparticles .....	126
4.1.1(d)	Entrapment Efficiency (EE) of TQ-PLGA-PF68 Nanoparticles .....	126
4.1.1(e)	<i>In vitro</i> Cumulative TQ Release .....	130
4.1.2	Biological Evaluation of TQ-PLGA-PF68 Nanoparticles .....	132
4.1.2(a)	Cell Viability Assay.....	132
4.1.2(b)	Colony Formation Assay .....	136
4.1.2(c)	Scratch-Wound Healing Assay .....	138
4.1.2(d)	Effects of TQ-PLGA-PF68 Nanoparticles on P-gp Cell Surface Expression.....	142
4.1.2(e)	Rh123 Efflux Assay.....	144

4.1.3	TUNEL Assay .....	146
4.1.4	TEM Observation of TQ-PLGA-PF68 Nanoparticles in TamR MCF 7 Cells .....	153
4.2	Discussion .....	155
4.3	Conclusion.....	166
<b>CHAPTER 5</b>	<b>MOLECULAR EFFECTS OF TQ-PLGA-PF68 NANOPARTICLES ON DRUG RESISTANT BREAST CANCER CELL MODEL.....</b>	<b>167</b>
5.1	Results .....	167
5.1.1	RT <sup>2</sup> Profiler PCR Array Analysis .....	167
	5.1.1(a) Sample Purity.....	168
	5.1.1(b) Quality Control (QC).....	171
	5.1.1(c) Data Analysis.....	171
5.1.2	KEGG Analysis.....	177
5.1.3	Functional Importance Analysis of MDR1, NF-κB and p21 Waf1/Cip1 Expression in TamR MCF 7 Cells. ....	178
5.2	Discussion .....	185
5.3	Conclusion.....	193
<b>CHAPTER 6</b>	<b>GENERAL DISCUSSION .....</b>	<b>194</b>
<b>CHAPTER 7</b>	<b>CONCLUSION, STUDY LIMITATIONS AND FUTURE RECOMMENDATIONS.....</b>	<b>205</b>
7.1	General Conclusion .....	205
7.2	Study Limitations .....	209
7.3	Future Recommendations.....	210
<b>REFERENCES</b>	<b>.....</b>	<b>212</b>
<b>APPENDICES</b>		
<b>PUBLICATION</b>		
<b>CONFERENCE</b>		

## LIST OF TABLES

	<b>Page</b>
Table 1.1	2013 St. Gallen - Breast cancer subtypes classification.....3
Table 1.2	Taxonomic group of <i>Nigella sativa</i> (NCBI: txid555479) ..... 14
Table 1.3	Selection criteria for a nanoparticulate-based therapeutic platform. .....20
Table 1.4	List of nanomedicines as breast cancer therapeutics approved by the U.S. FDA and those in clinical trials. ....22
Table 1.5	Anticancer agent of plant origin for breast cancer therapeutics. ....31
Table 1.6	Examples of camptothecins nanomedicine for breast cancer treatment in clinical trial.....34
Table 1.7	Example of preclinical approach of TQ nanomedicines for breast cancer treatment.....37
Table 1.8	Free TQ in clinical trial. ....39
Table 2.1	List of solvents. ....47
Table 2.2	List of chemicals and reagents. ....47
Table 2.3	List of drug chemotherapy and endocrine drugs. ....48
Table 2.4	List of cell culture reagents. ....49
Table 2.5	List of primary antibodies. ....49
Table 2.6	List of secondary antibodies.....49
Table 2.7	List of assay kits. ....50
Table 2.8	List of software.....50
Table 2.9	List of chemical compositions used in the TQ-Np formulations with different percentage of surfactant. ....60
Table 2.10	The PDI values for different classes of nanoparticles dispersity. ....62
Table 2.11	Range of the zeta potential value of the nanoparticles. ....62
Table 2.12	Compendial dissolution media used to simulate the pH conditions in gastrointestinal tract. ....65

Table 2.13	List of parental and resistant breast cancer cell lines. ....	66
Table 2.14	Composition of rTdT incubation buffer mixture.....	75
Table 2.15	Fixation, embedding and cross-sectioning protocol of TamR MCF 7 cells treated with TQ-PLGA-PF68 nanoparticles.....	78
Table 2.16	Genomic DNA elimination mixture. ....	82
Table 2.17	Reverse-transcription mixture. ....	83
Table 2.18	List of target genes and housekeeping genes. ....	84
Table 2.19	Layout of Custom RT <sup>2</sup> Profiler PCR array.....	85
Table 2.20	PCR components mixture.....	86
Table 2.21	Standard cycling amplification for 40 cycles.....	86
Table 2.22	Different BSA protein concentration as standard for Bradford assay. ....	90
Table 2.23	Electrophoresis and electrotransfer conditions of proteins studied.....	91
Table 2.24	Dilution ratio of primary and secondary antibodies.....	93
Table 3.1	IC <sub>50</sub> value of each of parental cell lines at different time points. ....	98
Table 3.2	Dose of anticancer drug in development of resistant subtypes with acquired resistance.....	100
Table 3.3	Resistant Index (RI) and classification of the cell lines after treatment with anticancer drugs into resistant cell lines.....	102
Table 3.4	Comparison of Rh123 retention between the parental and resistant subtypes.....	107
Table 4.1	FTIR analysis of functional groups present in compounds studied.....	121
Table 5.1	Sample RNA concentration and purity.....	169
Table 5.2	Summary of genes and fold change from Profiler PCR array analysis for treated TamR MCF 7 cells with TQ-PLGA-PF68 nanoparticles.....	174

Table 5.3	The significant KEGG pathways enriched by the 18 downregulated genes in TamR MCF 7 cells after treatment with TQ-PLGA-PF68 nanoparticles.....	177
Table 5.4	Percentage (%) of cells expressing p21 Waf1/Cip1 in different cell cycle phases in untreated and treated TamR MCF 7 cells.....	184

## LIST OF FIGURES

	<b>Page</b>
Figure 1.1	Chemical structure of tamoxifen. PubChem CID=2733526. <a href="https://pubchem.ncbi.nlm.nih.gov/compound/Tamoxifen">https://pubchem.ncbi.nlm.nih.gov/compound/Tamoxifen</a> . Created with BioRender.com. .... 7
Figure 1.2	Major metabolic pathways for tamoxifen and the main cytochrome P450 (CYP) enzymes involved with the capacity of ER binding. Created with BioRender.com. .... 8
Figure 1.3	Schematic diagram shows tamoxifen binding to oestrogen receptor and prevention of oestrogen to its receptor (adapted from <a href="https://www.riverpharmacy.ca">https://www.riverpharmacy.ca</a> ). Created with BioRender.com. .... 9
Figure 1.4	Multiple mechanisms that are involved in the development of resistance to therapeutic agents. Created with BioRender.com. .... 11
Figure 1.5	<i>Nigella sativa</i> flower (A) and black seeds (B). (Adapted from <a href="http://bioweb.uwlax.edu/bio203/">http://bioweb.uwlax.edu/bio203/</a> )..... 13
Figure 1.6	Chemical structure of TQ. PubChem SID=386221103. ( <a href="https://pubchem.ncbi.nlm.nih.gov/substance/386221103">https://pubchem.ncbi.nlm.nih.gov/substance/386221103</a> ). Created with BioRender.com ..... 15
Figure 1.7	Multitargeted protective effects of TQ mechanism against drug-resistant breast cancer. Created with BioRender.com. .... 18
Figure 1.8	Nanoparticulate-based chemotherapeutic delivery platforms approved by the US FDA for cancer treatment. (A) Liposomes are spherical vesicle composed of an aqueous core and a membranous lipid bilayer, preferable for encapsulation of hydrophilic drugs; (B) Nanoparticle albumin-bound paclitaxel (Nab-paclitaxel) is a colloid suspension of paclitaxel; (C) Polymeric nanoparticles are self-assembled from amphiphilic and biodegradable polymers in aqueous solution and are effective to encapsulate hydrophobic drugs. Created with BioRender.com. .... 24
Figure 1.9	A general chemical structure of poloxamer. Created with BioRender.com. .... 29

Figure 2.1	Experimental flow chart of the study. Created with BioRender.com.....	51
Figure 2.2	Flow chart of steps in TUNEL assay with flow cytometry method...73	
Figure 2.3	Flow chart of steps in TUNEL assay to be visualised by fluorescence microscopy. ....	76
Figure 3.1	MTS assay for determination of half-maximal inhibitory (IC <sub>50</sub> ) concentration. Cell viability profile of MCF 7 (A), UACC 732 (B) and MDA-MB 231 (C). To determine IC <sub>50</sub> , cells were treated with respective drugs with various concentration for 24, 48 and 72 hours. The significant difference was determined by two-way ANOVA and followed by Bonferroni post-hoc test for multiple comparison (times and concentrations). Data is presented as mean±SD of three separate experiments. ....	99
Figure 3.2	Semi-logarithmic histogram of P-gp cell surface expression in parental and respective resistant phenotype cell lines by flow cytometric method. MCF 7-P (A); UACC 732-P (B); MDA-MB 231-P (C); TamR MCF 7 (D); TamR UACC 732 (E); PacR MDA-MB 231 (F); Green line indicated the negative control of the unstained cells with anti P-gp PE antibody; purple-coloured area indicated the cell lines with anti P-gp PE antibody staining. ....	104
Figure 3.3	Bar graph represent quantification of P-gp cell surface expression from flow cytometry analyses. Comparison was done between parent and resistant subtypes using t-test. Data is presented as mean±SD of three separate experiment.....	105
Figure 3.4	P-gp efflux activity in parental and resistant cell lines. Flow cytometric histogram of Rh123 stained parental (green line) and resistant (purple area) cells. MCF 7-P and TamR MCF 7 (A); UACC 732-P and TamR UACC 732 (B); MDA-MB 231-P and PacR MDA-MB 231 (C). Bar graph represents intracellular accumulation of Rhodamine 123 in each of the cells (D, E, F).....	108
Figure 3.5	Phase contrast microscopic image of morphological changes of MCF 7 parental breast cancer cell line and the respective	

	tamoxifen-resistant subtypes. MCF 7-P (A); TamR MCF 7 (B). Cells were observed at 400× magnification with scale bar 20 μm... 110
Figure 3.6	Phase contrast microscopic image of morphological changes of UACC 732 parental breast cancer cell line and the respective tamoxifen-resistant subtypes. UACC 732-P (A); TamR UACC 732 (B). Cells were observed at 400× magnification with scale bar 20 μm..... 111
Figure 3.7	Phase contrast microscopic image of morphological changes of MDA-MB 231 parental breast cancer cell line and the respective paclitaxel-resistant subtypes. MDA-MB 231-P (A); PacR MDA-MB 231 (B). Cells were observed at 400× magnification with scale bar 20 μm..... 112
Figure 4.1	FTIR spectrum of compound TQ-PLGA-PF68 nanoparticles. .... 120
Figure 4.2	Graph shows difference in ZP (A) and particle size (B) of TQ-PLGA-PF68 with pH. The significant difference was determined by one-way ANOVA. Data is presented as mean±SD of three separate experiment. .... 125
Figure 4.3	Particle size distribution and particle structure of TQ-PLGA-PF68 nanoparticles. Particle size distribution of TQ-PLGA-PF68 nanoparticles with average size at 76.92±27.38 nm, processed by Microcal Origin 6 software (Origin Lab, United States) (A); TQ-PLGA-PF68 nanoparticle image observation at 10,000× magnification with scale bar 500 nm using FEI CM12 transmission electron microscopy (Thermo Fisher Scientific, Oregon, United States) (B). .... 127
Figure 4.4	Percentage of encapsulation efficiency of TQ-PLGA-PF68 nanoparticles by varying concentration of Pluronic F68 (% w/v). Significant difference was $P<0.001$ , performed using one-way ANOVA, n=3, mean±SD. .... 129
Figure 4.5	Release profiles of TQ-PLGA-PF68 nanoparticles formulation in simulated gastrointestinal tract. .... 131

- Figure 4.6 Cell viability effects of TQ-PLGA-PF68, vinblastine (Vb) and paclitaxel (PAC) was determined by MTS assays on parental and resistant subtype cell lines. Cells were treated accordingly for 72 hours to assess the cell viability. The significant difference was determined by two-way ANOVA. Data is presented as mean±SD of three separate experiment..... 134
- Figure 4.7 Bar chart represent the potential of TQ-PLGA-PF68 nanoparticles to inhibit colony formation of TamR MCF 7 cells. Percentage of surviving fraction of TamR MCF 7 cells seeded at low density (25 cells/well) after 72 hours of TQ-PLGA-PF68 treatment (IC<sub>50</sub> value) followed by 12 days incubation without TQ-PLGA-PF68 nanoparticles. Results are expressed as mean±SD of three separate experiments. Significant difference is presented as \*\**P*<0.001 by t-test. (-, treatment without TQ-PLGA-PF68; +, treatment with TQ-PLGA-PF68)..... 137
- Figure 4.8 TQ-PLGA-PF68 nanoparticles induces anti-migratory effect in the TamR MCF 7 cells. Phase contrast microscopic images of scratch-wound assay on TamR MCF 7 cells (A). TamR MCF 7 cells was treated with TQ-PLGA-PF68 nanoparticles (IC<sub>50</sub>=96.34 µg/mL) and images were captured at 0 hour (T0), 12 hours (T12) and 24 hours (T24). Cells were observed at 100× magnification with scale bar 100 µm. Bar graphs represent percentage of wound closure area after 12 hours of TQ-PLGA-PF68 nanoparticles treatment in TamR MCF 7 cells (B). T-test was performed, \**P*<0.05, mean±SD, n=3.. 140
- Figure 4.9 Scatter plot displays closure area of the wound over time and the rate of wound closure in untreated and treated TamR MCF 7 cells. TamR MCF 7 cells was treated with TQ-PLGA-PF68 nanoparticles (IC<sub>50</sub>=96.34 µg/mL). A linear regression was run on the wound closure data using the GraphPad Prism software (version 5.0, GraphPad Software, Inc.) to generate the *r*<sup>2</sup> value and rate of closure. .... 141

- Figure 4.10 P-gp expression analysed with flow cytometer in TamR MCF 7 cells before and after treatment with TQ-PLGA-PF68 nanoparticles ( $IC_{50}$  value=96.34  $\mu\text{g/mL}$ ). Flow cytometric histogram depicts the P-gp expression (A). Bar graph represents the fluorescence index of P-gp expression obtained from flow cytometry data (B). Results are expressed as mean $\pm$ SD of three separate experiments. Significance difference was determined by t-test ( $P<0.05$ )..... 143
- Figure 4.11 Rh123 efflux in TamR MCF 7 cells. Flow cytometric histogram of the intracellular retention of Rh123 in TamR MCF 7 cells (A). Flow cytometric analysis of Rh123 efflux in TamR MCF 7 cells (B). TamR MCF 7 cells were treated with 96.34  $\mu\text{g/mL}$  TQ-PLGA-PF68 nanoparticles (TQ-PLGA-PF68<sup>+</sup>) or without TQ-PLGA-PF68 nanoparticles (TQ-PLGA-PF68<sup>-</sup>) and incubated for 72 hours. Two-way ANOVA was performed for  $P<0.05$ . All experiments were done in triplicates..... 145
- Figure 4.12 TUNEL assay graphical representation of the percentage of the number of apoptotic cells in TamR MCF 7 cells measured at 6 hours, 24 hours, 48 hours and 72 hours by flow cytometry. The histogram shows the relative proportion of TUNEL-positive cells in different time course. Significantly different of TQ-PLGA-PF68 treated samples ( $P<0.0001$ ) was analysed using one-way ANOVA followed by Tukey's multiple comparison tests,  $n=3$ . ..... 148
- Figure 4.13 Histogram of cell cycle assay in TamR MCF 7 cells. A number of cells in gated population G0/G1, S and G2/M phases of the cell cycle after 6, 24, 48 and 72 hours. Percentage of cells under each area was quantified by using the Modfit software (BD Bioscience, United States). Analysis was performed using two-way ANOVA with respect to untreated TamR MCF 7 cells (left bar),  $n=3$ ..... 149
- Figure 4.14 Fluorescence visualization of untreated and treated TamR MCF 7 cells labelled with TUNEL stain (green fluorescence) and counterstained with DAPI (blue) . Negative control=incubation

	buffer without rTDT enzyme; Positive control=10 units/mL DNase I; TQ-PLGA-PF68 <sup>-</sup> = untreated TamR MCF 7 cells; TQ-PLGA-PF68 <sup>+</sup> = treated TamR MCF 7 cells with 96.34 µg/mL of TQ-PLGA-PF68 nanoparticles for 72 hours. Red arrows: cells exhibit nuclear condensation of the cells; Purple arrows: membrane blebbing of the cells. Cells were observed at 400× magnification with scale bar 20 µm. ....	152
Figure 4.15	TEM images of TamR MCF 7 treated with TQ-PLGA-PF68 nanoparticles for 72 hours. Red arrows indicate the presence of TQ-PLGA-PF68 nanoparticles inside the cells. Green arrows, cell is demonstrating blebbing and swelling. Cells were observed at 2000× magnification with scale bar 2 µm. Labels: N, nucleus; C, chromatin; C-R, chromatin-reduced nuclear area. ....	154
Figure 5.1	Agarose gel (1%, w/v) electrophoresis of total RNA extracted from untreated and treated TamR MCF 7 cells with TQ-PLGA-PF68 nanoparticles. Lane 1-3: Untreated TamR MCF 7 cells; Lane 4-5: Treated TamR MCF 7 cells with TQ-PLGA-PF68 nanoparticles....	170
Figure 5.2	Volcano plot indicating the differentially expressed genes. Analysis was performed with the Custom RT <sup>2</sup> Profiler PCR array, CAPA9632-12: CLAH23537. Twenty-six genes of breast cancer-related genes were analysed using RT <sup>2</sup> Profiler PCR Array Data Analysis Webportal, <a href="https://dataanalysis2.qiagen.com/pcr/analysis/26530">https://dataanalysis2.qiagen.com/pcr/analysis/26530</a> (Qiagen, United States). A cut-off value of 2 was used to indicate differentially expressed genes ( $P>0.05$ , $n=3$ )......	173
Figure 5.3	Difference in gene expression before and after treatment with TQ-PLGA-PF68 nanoparticles. Dendrogram shows the hierarchical clustering and heat map. Each row represents a gene. Red and green represent high and low expression levels, respectively.....	176
Figure 5.4	Expression of MDR1 in TamR MCF 7 cells. Immunoblot analysis of TamR MCF 7 cells before and after treatment with TQ-PLGA-PF68 nanoparticles. Whole cell lysates from cell culture were	

	resolved on 10% SDS-polyacrylamide gel and transferred to a PVDF membrane. Whole cells lysate from untreated cells was used as control. MDR1 was detected using the monoclonal antibody (1:750 dilution). HRP conjugated secondary antibody was used and images were taken using Biorad gel doc instrument (n=3; T-test, $P>0.05$ ).....	181
Figure 5.5	Expression of NF- $\kappa$ B in TamR MCF 7 cells. Immunoblot analysis of TamR MCF 7 cells before and after treatment with TQ-PLGA-PF68 nanoparticles. Whole cell lysates from cell culture were resolved on 10% SDS-polyacrylamide gel and transferred to a PVDF membrane. Whole cells lysate from untreated cells was used as control. NF- $\kappa$ B was detected using the monoclonal antibody (1:750 dilution). HRP conjugated secondary antibody was used and images were taken using Biorad gel doc instrument (n=3; T-test, $P>0.05$ ).....	182
Figure 5.6	Flow cytometry analysis of p21 Waf1/Cip1 distribution in TamR MCF 7 cells. (n=3, T-test, $P<0.05$ ). All experiments were performed in triplicates.....	183
Figure 5.7	Inhibitory potential of TQ-PLGA-PF68 nanoparticles on the tamoxifen metabolism pathway-cytochrome P450. Created with BioRender.com.....	187
Figure 5.8	Illustration of TQ-PLGA-PF68 nanoparticles entrance into TamR MCF 7 cells. TQ was released from its nanoparticles core and indirectly inhibit the ABCB1 and ABCG2 transporters. Consequently, accumulation of TQ inside the cells would induce cell apoptosis. Created with BioRender.com. ....	190
Figure 5.9	NF- $\kappa$ B target genes involved in cancer biological functions. NF- $\kappa$ B activation affects all six hallmarks of cancer through the transcription of genes involved in cell proliferation, angiogenesis, metastasis, inflammations, and suppression of apoptosis. (Adapted from Baud & Karin, 2009; Li & Sethi, 2010) .....	191

Figure 6.1	Stages of evolvement from parent MCF 7 to tamoxifen resistant MCF 7 cell line. Acquired resistance with gradual increase in drug dose developed cells with different levels of resistance over time. .197
Figure 6.2	Schematic diagram depicting TQ nanoparticle formulations by emulsification solvent-evaporation technique. TQ self-assembles with amphiphilic molecule of Pluronics F68 and PLGA-PEG forming hydrophobic core while intact TQ is located within the core (A). TEM observation of a TQ nanoparticles (B). Created with BioRender.com. ....200
Figure 6.3	Schematic representation of TQ-PLGA-PF68 nanoparticles drug delivery mechanism in tamoxifen-resistant breast cancer cells. Internalisation of TQ-PLGA-PF68 nanoparticles may occur through receptor-mediated endocytosis and TQ is released in cytoplasm by lysosomal degradation. Polymeric PLGA could overcome tamoxifen resistant in ER positive breast cancer cells by activating proapoptotic mediator involved in cancer hallmark (Modified from Santosh <i>et al.</i> , 2017; Upadhyay <i>et al.</i> , 2019). Abbreviation: ER+ BC, oestrogen receptor positive breast cancer; TQ, thymoquinone. Created with BioRender.com. ....203

## LIST OF SYMBOLS

°C	Degree Celsius
μg	Microgram
μg/mL	Microgram per milliliter
μM	Micromolar
CO <sub>2</sub>	Carbon dioxide
g	Gravity
G0	Gap G0 growth phase
G1	Gap G1 growth phase
G2	Gap G2 growth phase
IC <sub>50</sub>	Inhibitory concentration 50%
L	Liter
M	Molar
mg/mL	Milligram per milliliter
mL	Milliliter
mM	Milimolar
nM	Nanomolar
OD	Optical density
RPM	Revolution per minute
s	singlet
SD	Standard deviation
w/v	Weight per volume

## LIST OF ABBREVIATIONS

4-OHT	4-hydroxytamoxifen
AIC	Anthracycline-induced cardiotoxicity
BSA	Bovine serum albumin
BSC	Breast-conserving surgery
BME	$\beta$ -mercaptoethanol
CYP450	Cytochrome P450
DCM	Dichloromethane
DMSO	Dimethyl sulfoxide
EE	Encapsulation efficiency
EMA	European Medicines Agency
EMT	Epithelial-mesenchymal transition
ER	Oestrogen receptor
FBS	Fetal bovine serum
GCB	Gemcitabine
GIT	Gastrointestinal tract
HCl	Hydrochloric acid
HER2	Human epidermal growth receptor
MDR	Multidrug resistant
MRP	Multidrug resistance protein
Nab	Nanoparticle albumin-bound
NF- $\kappa$ B	nuclear factor- $\kappa$ B
NCCN	National Comprehensive Cancer Network
NSCLC	Non-small cell lung cancer
PBS	Phosphate-buffered saline
PCL	Poly (caprolactone)

PEO	Poly (ethylene oxide)
P-gp	P-glycoprotein
PLA	Poly (lactic acid)
PLGA	Poly lactic-co-glycolic acid
PLGA-PEG	Poly lactic-co-glycolide-block-poly (ethylene glycol)
PPO	Poly (propylene oxide)
PR	Progesterone receptor
qRT-PCR	Quantitative Reverse Transcription Polymerase Chain Reaction
Rh123	Rhodamine 123
RI	Resistance index
RPMI 1640	Roswell Park Memorial Institute 1640
SDS	Sodium dodecyl sulphate
SERMs	Selective oestrogen receptor modulators
siRNA	Small interfering RNA
SLNs	Solid lipid nanoparticles
TEM	Transmission electron microscope
TFs	Transcription factors
TNBC	Triple negative breast cancer
TQ	Thymoquinone
U.S. FDA	U.S. Food and Drug Administration

## **LIST OF APPENDICES**

APPENDIX A	COLONY-FORMING ASSAY OPTIMIZATION
APPENDIX B	GEL PREPARATION
APPENDIX C	DATA QUALITY CONTROL (QC)
APPENDIX D	Ct VALUE DATA

**KAJIAN AKTIVITI PENCEGAHKEMO KANSER BAGI FABRIKASI  
NANOPARTIKEL BERKAPSULKAN TQ DENGAN PF68-PLGA  
TERHADAP TITISAN SEL KANSER PAYUDARA TERPILIH**

**ABSTRAK**

Kerintangan ubat ialah halangan utama dalam terapi kanser payudara. Oleh itu, beberapa kajian telah dijalankan untuk mengatasi masalah ini dengan menggunakan sebatian bioaktif. Thymoquinone (TQ) telah dikaji secara meluas untuk ciri-ciri antikansernya. Dalam keadaan klinikal, potensi terapinya belum diterokai kerana sifatnya yang tidak stabil. Lantaran itu, objektif kajian ini menyasarkan kepada sintesis nanopartikel polimer yang mengandungi TQ untuk mengatasi masalah ini. Tiga jenis sel kanser payudara (MCF 7, UACC 732, MDA-MB 231) yang menunjukkan kerintangan ubat telah dihasilkan menggunakan kaedah *'pulse method'*. Sintesis nanopartikel TQ telah dilakukan dengan menggunakan teknik penyejatan-pelarut emulsi (*emulsion-solvent evaporation*) campuran polimer poly(L-lactide-co-glycolide)-b-poly(ethylene glycol) dan Pluronic F68. Ciri-ciri nanopartikel TQ ini ditentukan menggunakan FTIR, taburan saiz, morfologi, kecekapan enkapsulasi (*encapsulation efficiency*) dan kajian pelepasan (*drug release study*) TQ. Pengesanan indeks rintangan (RI) dilakukan dengan cerakinan MTS, penghasilan P-glycoprotein dan kecerakinan pengaliran keluar ubat. Kesan-kesan anticancer nanopartikel TQ-PLGA-PF68 dikaji menggunakan analisis fungsian, cerakinan TUNEL, qRT-PCR dan kaedah Western blot. Saiz nanopartikel TQ-PLGA-PF68 ialah <100 nm, bulat dengan pengkapsulan jelas TQ dalam teras berdasarkan pemerhatian FTIR and TEM. Ia mempunyai kecekapan pengkapsulan (94%) dan pelepasan TQ >50% dalam keadaan

berasid. RI terhadap tamoksifen bagi sel TamR MCF 7 ialah 2.32 kali ganda dan 1.32 kali ganda pada TamR UACC 732 dan 1.59 kali ganda pada PacR MDA-MB 231 terhadap paclitaxel. Analisis lanjut telah dilakukan dengan TamR MCF 7 memandangkan ia kanser payudara paling tersebar luas dan menunjukkan rintangan lebih tinggi kepada kemoterapi standard. Cerakinan TUNEL menunjukkan bahawa nanopartikel TQ-PLGA-PF68 menggalakkan apoptosis dalam sel TamR MCF 7 ( $P < 0.0001$ ) dan penghentian kitaran sel di fasa S. Penghasilan P-gp adalah 33 kali ganda lebih rendah dalam sel TamR MCF 7 selepas dirawat dengan nanopartikel TQ-PLGA-PF68 ( $P < 0.05$ ). Ini telah disokong oleh cerakinan pengaliran keluar yang menunjukkan pengumpulan intrasel Rhodamine 123 ( $P < 0.05$ ). Analisis sitotoksikan menunjukkan perencatan perkembangbiakan sel (nilai  $IC_{50} = 96.34 \mu\text{g/mL}$ ;  $P < 0.05$ ). Ini disokong oleh kajian fungsian, di mana perencatan pembentukan koloni ( $P < 0.05$ ) dan penghijrahan ( $P < 0.05$ ). Analisis lanjut menunjukkan penurunan dalam ekspresi gen yang terlibat dalam kerintangan ubat, mekanisme kitar sel dan apoptosis (*ABCG2, CYP1A1, CYP2B6, CYPC19, CYP2D6, CYP3A4, CYP3A5, SULT1E1, BRCA1, CDKN1A, CDKN2A, EGFR, NF- $\kappa$ B1, SULT1A1, UGT2B1, ABCC2, CDKN1B*). Analisis KEGG menunjukkan hubungan kepada beberapa jaringan lain yang berhubung kait dengan laluan pengisyaratan rintangan (*resistance signaling pathway*) ( $P < 0.05$ ). Analisis proteomik mengesahkan penurunan ekspresi, P-gp ( $P > 0.05$ ) dan pengisyaratan hilirnya (*downstream signaling*) melibatkan protein NF- $\kappa$ B ( $P > 0.05$ ) and p21 ( $P < 0.05$ ). Penemuan mencadangkan rawatan menggunakan nanopartikel TQ-PLGA-PF68 boleh mengurangkan mekanisme-mekanisme kerintangan ubat oleh sel kanser payudara dari kumpulan reseptor oestrogen positif.

**INVESTIGATION ON CANCER CHEMOPREVENTIVE ACTIVITY OF  
FABRICATED TQ ENCAPSULATED PLGA-PF68 NANOPARTICLES ON  
SELECTED BREAST CANCER CELL LINES**

**ABSTRACT**

Drug resistance is remains as a major obstacle in breast cancer therapy. This has attracted considerable interest to overcome drug resistance with bioactive compounds. Free thymoquinone (TQ) has been extensively studied for its anticancer properties. In the clinical setting, its therapeutic potential has not been explored due to its volatile nature. Therefore, the study aimed to develop TQ polymeric nanoparticles and evaluate its effects on drug resistant breast cancer cells. Development of drug resistant breast cancer subtype (MCF 7, UACC 732, MDA-MB 231) were done using pulse method. Synthesis of nanoparticles was done by encapsulating TQ with polymeric poly(L-lactide-co-glycolide)-b-poly(ethylene glycol) and Pluronic F68 using emulsion-solvent evaporation technique and characterised using FTIR spectroscopic study, size distributions, morphology, entrapment efficiency, and drug release study. Confirmation of resistance index (RI) was performed with MTS assay, P-glycoprotein expression and efflux assay. Anticancer effects were studied using functional analysis, TUNEL assay, qRT-PCR array and Western blot method. Size of TQ-PLGA-PF68 nanoparticles was <100 nm, spherical with confirmed encapsulation of TQ within core based on FTIR and TEM observation. It had high encapsulation (94%) and drug release of >50% at acidic conditions. RI of TamR MCF 7 cells was 2.32-fold and 1.32-fold in TamR UACC 732 to tamoxifen and 1.59-fold in PacR MDA-MB 231 to paclitaxel. Further analysis was done with TamR MCF 7 as it is the most prevalent breast cancer and exhibited higher resistance to standard

chemotherapy. TUNEL assay indicated that TQ-PLGA-PF68 nanoparticles induced apoptosis in TamR MCF 7 cells was time dependant ( $P<0.0001$ ) and arrest of cells at S-phase. P-gp expression was 33-fold lower in TamR MCF 7 cells after treatment with TQ-PLGA-PF68 nanoparticles ( $P<0.05$ ). This was supported by efflux assay which exhibited intracellular accumulation of Rhodamine 123 ( $P<0.05$ ). Cytotoxicity analysis exhibited significant inhibition of cell proliferation ( $IC_{50}$  value=96.34  $\mu$ g/mL;  $P<0.05$ ). This is supported by functional study, where inhibition of colony formation ( $P<0.05$ ) and migration ( $P<0.05$ ) were noted. Further analysis on relative gene expression provides evidence of downregulation of genes involved in drug resistance, cell cycle and apoptosis mechanisms (*ABCG2*, *CYP1A1*, *CYP2B6*, *CYPC19*, *CYP2D6*, *CYP3A4*, *CYP3A5*, *SULT1E1*, *BRCA1*, *CDKN1A*, *CDKN2A*, *EGFR*, *NF- $\kappa$ B1*, *SULT1A1*, *UGT2B1*, *ABCC2*, *CDKN1B*). KEGG analysis showed link to several resistance signaling pathways ( $P<0.05$ ). Finally, proteomic analysis confirmed the downregulation of P-gp ( $P>0.05$ ) and its downstream signaling involving NF- $\kappa$ B ( $P>0.05$ ) and p21 proteins ( $P<0.05$ ). Findings suggest TQ-PLGA-PF68 nanoparticles treatment could mitigate drug resistant mechanisms of oestrogen receptor positive breast cancer cells.

# CHAPTER 1

## INTRODUCTION

### 1.1 Breast Cancer: An Overview

Cancer is defined as the unregulated proliferation of cancer cells by dividing continuously and have the capability of invading other tissues or organs (Pugazhendhi *et al.*, 2018). Cancer can arise almost anywhere in the body. It is characterised as carcinoma (originates from the epithelial cells i.e. breast cancer), sarcoma (arise from connective tissue i.e. osteosarcoma), lymphoma (originates from the lymph nodes) and leukaemia (immature blood cells that grow in the bone marrow) (Zhou *et al.*, 2012).

Globally, breast cancer is one of the most common cancer and is the highest incidence of cancer-related death among women (Siegel *et al.*, 2018). Breast cancer affects more than 2 million women annually. In 2018, it was reported that 627,000 (15%) women died from breast cancer (WHO, 2018). In Malaysia, breast cancer is the most commonly diagnosed cancer among Malaysian women regardless of their backgrounds and it is also the main cause of cancer death in Malaysia women (Bray *et al.*, 2018).

Breast cancer subtypes are classified based on pathological biomarkers. There are four breast cancer subtypes and defined by the expression of oestrogen receptor (ER), progesterone receptor (PR) and overexpression of human epidermal growth receptor (HER2) as shown in Table 1.1. They are classified into luminal A subtype (ER+/PR+/HER2-) that makes up approximately 50-60% of breast cancers which are slow-growing and less aggressive (Perou & Borresen-Dale, 2011; Yersal & Barutca,

2014; Dai *et al.*, 2017). The luminal B subtype (ER+/PR+/HER2+) represents 15-20% of breast cancers and exhibit more aggressive phenotype compared to luminal A subtype (Perou & Borresen-Dale, 2011; Yersal & Barutca, 2014; Dai *et al.*, 2017). Meanwhile, HER2 positive subtype (ER-/PR-/HER2+) accounts for 15-20% of breast cancer subtypes, which are highly invasive and aggressive in terms of biological and clinical behaviour (Yersal & Barutca, 2014; Dai *et al.*, 2017; Vernieri *et al.*, 2019). While, 10-20% of breast cancer is basal-like, which is referred as triple negative breast cancer (TNBC) that ER-, PR-, and does not overexpress HER2 (Perou & Borresen-Dale, 2011; Dai *et al.*, 2017). Generally, it has the worse prognosis of all sub-types (Sprouse & Herbert, 2014). Meanwhile, the Ki-67 is a cell proliferation marker and present only during the active phases of the cell cycle. Proliferation is a key feature of the progression of tumours (Urruticoechea *et al.*, 2005). High levels of Ki-67 indicate cells that are actively proliferating, thus are prone to mutation initiation and expansion. In breast cancer, a result of Ki-67 less than 10% is considered low, 10-20% borderline, and high if more than 20%.

In United States, it was reported that between 2012-2016, the breast cancer luminal A subtype is the common subtype with the prevalence of 85 new cases per 100,000 women (Fallahpour *et al.*, 2017). Meanwhile, an increasing trend is seen in Malaysia. The luminal A subtype rate increased by 2% in every five-year cohort, where it increased from 54.5% in 1994–1998, to 56.4% in 1999–2003 and 58.4% in 2004–2008 (Yip *et al.*, 2011). Unlike, the rate of HER2 positive breast cancer which remained constant.

**Table 1.1: 2013 St. Gallen - Breast cancer subtypes classification.**

Subtype	Characteristics		Medical therapy
Luminal A	ER PR HER2 Low Ki-67 (<14%)	++ + - 	Endocrine therapy
Luminal B	ER PR HER2  High Ki-67 (>40%)	+ +/- +/-  	Chemotherapy; Endocrine therapy; Anti-HER2 targeted therapy
HER2-positive	ER PR  HER2 High Ki-67	- -  ++	Chemotherapy; Anti-HER2 targeted therapy
Triple negative	ER PR HER2 High Ki-67	- - - 	Chemotherapy

(Nielsen *et al.*, 2004; Goldhirsch *et al.*, 2011)

Several factors may lead to the initiation of breast cancer, such as genetic abnormalities that affected the gene expression and mutation of the tumour suppressor genes. The oncogenes that are frequently deregulated in breast cancer includes *ErbB2*, *PI3KCA*, *MYC*, and *CCND1* (encodes cyclin D1) (Lee & Muller, 2012). Occurrence of mutations in the tumour suppressor genes *BRCA1*, *BRCA2*, and *p53* are also responsible for development of breast cancer (Lee & Muller, 2012). Mutation in oncogenes and in tumour suppressor genes can generate a clonal cell population with proliferative characteristics that leads to the induction of cancer (Basu, 2018).

Hormonal factor has an important role in breast cancer and is strongly linked with risk of ER positive PR positive breast cancer (Cotterchio *et al.*, 2003; Yue *et al.*, 2010). Women with increased exposure to oestrogen because of early menarche, late

menopause, long-term menopausal oestrogen therapy, and oestradiol ( $E_2$ ) levels have higher risk of breast cancer.

## 1.2 Breast Cancer Treatment

A mammary tumour develops when the cells that make up the breast tissue replicate abnormally. This caused the complexity of breast cancer mechanisms that demands for comprehensive therapies. For patients, treatments rely on the stage and subtype. Surgical removal of the tumour is the first choice in treatment of breast cancer. Due to this the treatment is done by surgery or radiotherapy. Subsequently, the treatment involves chemotherapy and endocrine therapies. This is done to lower the risk of relapse and improve overall survival. Meanwhile, the higher classification and inoperable tumours are normally treated with chemotherapy. It is addressed as neoadjuvant treatment, which aims to reduce the size of the tumours. This will be followed by surgical treatment. In breast cancer treatment, type of treatment will be based on the status of the axillary nodes, subtypes and menopausal state (Wesolowski & Ramaswamy, 2011). However, majority of the breast cancer patients would need multiple therapies because of acquired resistance towards chemotherapy, anti-HER2 therapy and endocrine therapy (Cree & Charlton, 2017). Around 75% of breast cancer patients are reported to express oestrogen alpha ( $ER\alpha$ ) (Piva *et al.*, 2014). Therefore, this has led to the strategy of inhibiting oestrogen signalling as a therapeutic approach. Despite development of targeted anti-oestrogen therapies for ER positive, approximately 30-50% of patients still encounter relapse (Szostakowska *et al.*, 2019). Studies have shown that almost 15% of them with early stage had developed signs of recurrence within five years on adjuvant setting with endocrine therapy (Dowsett *et al.*, 2012). By 15 years, the recurrence rate was as high as 30% (Dixon, 2014).

However, approximately 40% of patients presenting with metastatic ER-positive state would eventually develop resistance after 2 years of endocrine therapy (Dixon, 2014).

The molecular targeting of tamoxifen is directed towards oestrogen receptor and is the standard treatment for patients expressing ER-positive (Manna & Holz, 2016). Interestingly, about 10% of patients with ER-negative breast cancers have responded to tamoxifen treatment (Manna & Holz, 2016). Numerous reports have found a significant fraction of women with ER-negative benefited from tamoxifen treatment (Radin & Patel, 2016).

For HER2 positive subtype, it has responded well to anti-HER2 therapies including trastuzumab and pertuzumab, lapatinib and the antibody-drug conjugate trastuzumab emtansine (Rinnerthaler *et al.*, 2019). Despite all these therapies, relapse is still reported to occur. This is because the HER2 metastatic ability in distant sites can counter the anti-HER2 targeting (Goel *et al.*, 2017; Vernieri *et al.*, 2019). Thus, resistance develops eventually, with primary or acquired resistance to anti-HER2 therapies is contributing most to the treatment failure (Wang & Dang, 2016; Vernieri *et al.*, 2019).

On the other hand, triple negative breast cancer (TNBC) is characterised by poor survival in comparison to the other breast cancer subtypes mainly due to absence of ER, PR and HER2 where targeted therapies towards ER and HER2 are ineffective in TNBCs. This subtype shows a higher tendency of relapse particularly in distant metastasis (Yuan *et al.*, 2014; Wahba & El-Hadaad, 2015). Moreover, resistance to chemotherapy is a major concern as treatment for TNBCs rely entirely on chemotherapy as standard of care (Sprouse, 2014; Nedeljković & Damjanović, 2019) and the respond of TNBCs towards chemotherapy is poor (Liedtke *et al.*, 2008).

Consequently, TNBCs patients often develop resistance (Nedeljković & Damjanović, 2019).

Furthermore, for many women with early breast cancer, breast-conserving surgery (BSC) is currently considered the best treatment option, followed by breast irradiation as recommended by National Comprehensive Cancer Network (NCCN) guidelines. This to destroy cancer cells that may not have been removed in the conserved breast tissue to prevent local recurrence and distant metastasis. Studies show that women who have BCS followed by radiation therapy have similar long-term survival rates as women who have a mastectomy. The likelihood of local relapse after breast conservations is low, at roughly 2-3% after 5 years (Nijenhuis & Rutgers, 2013). These techniques allow women with different forms of breast cancer to conserve their breasts.

### **1.3 Tamoxifen**

Tamoxifen (Figure 1.1), a selective oestrogen receptor modulators (SERMs) is currently prescribed for ER positive breast cancer (An, 2016). It was approved by the U.S. Food and Drug Administration (FDA) for the treatment of premenopausal women suffering from advanced breast cancer (Macgregor & Jordan, 1998; Hultsch, 2018). It is also used for treating man with breast cancer (Eggemann *et al.*, 2019). For the past three decades, tamoxifen has been used and significantly improved disease-free survival among breast cancer patients (Early Breast Cancer Trials Collaborative Group, 1992). Therefore, it has become the main hormonal therapy to prevent relapse among patient with ER-positive.

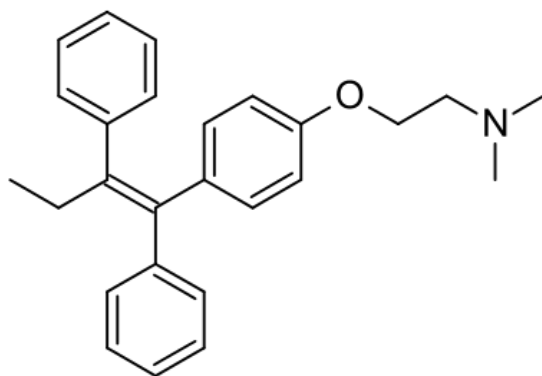


**Figure 1.1: Chemical structure of tamoxifen. PubChem CID=2733526. <https://pubchem.ncbi.nlm.nih.gov/compound/Tamoxifen>. Created with BioRender.com.**

### **1.3.1 Tamoxifen Metabolism**

Tamoxifen is a nonsteroidal triphenylethylene derivative that is metabolised by cytochrome P450 (CYP450) to form active metabolites such as 4-hydroxytamoxifen (4-OHT) and endoxifen (Figure 1.2). Principally, tamoxifen blocks oestrogen signalling in breast cancer cells and thus, inhibit ER activity associated with tumour cell growth (Dean, 2012) (Figure 1.3). The 4-OHT and endoxifen exhibit a 10-fold higher affinity to ER. They have 30 to 100-fold potency to inhibit cell proliferation of estrogen-dependent cells compared to tamoxifen. In fact, level of endoxifen in serum is more than 6-fold higher compared to 4-OHT (Higgins & Stearns, 2010). Thus, this provide evidence that endoxifen plays an important role for the activity of tamoxifen (Higgins & Stearns, 2010).

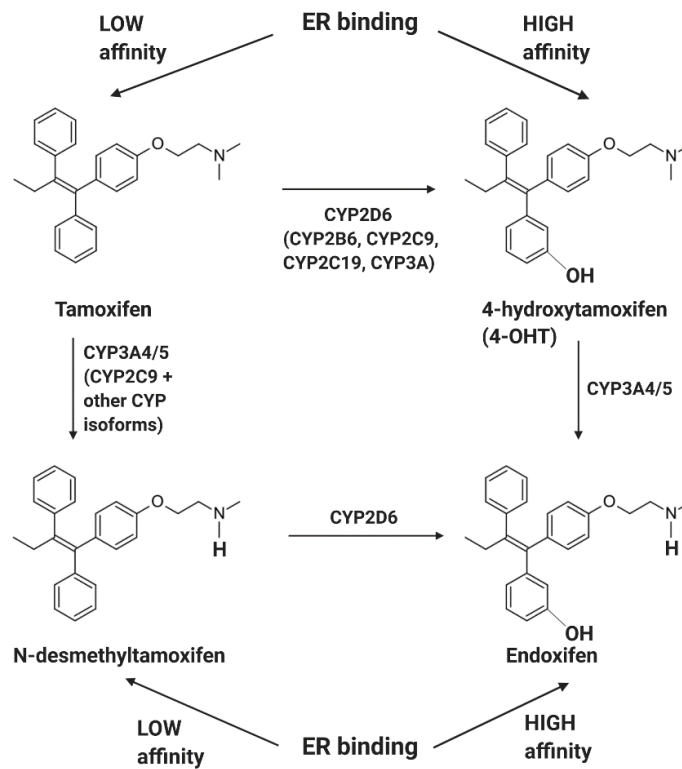


**Figure 1.2: Major metabolic pathways for tamoxifen and the main cytochrome P450 (CYP) enzymes involved with the capacity of ER binding. Created with BioRender.com.**

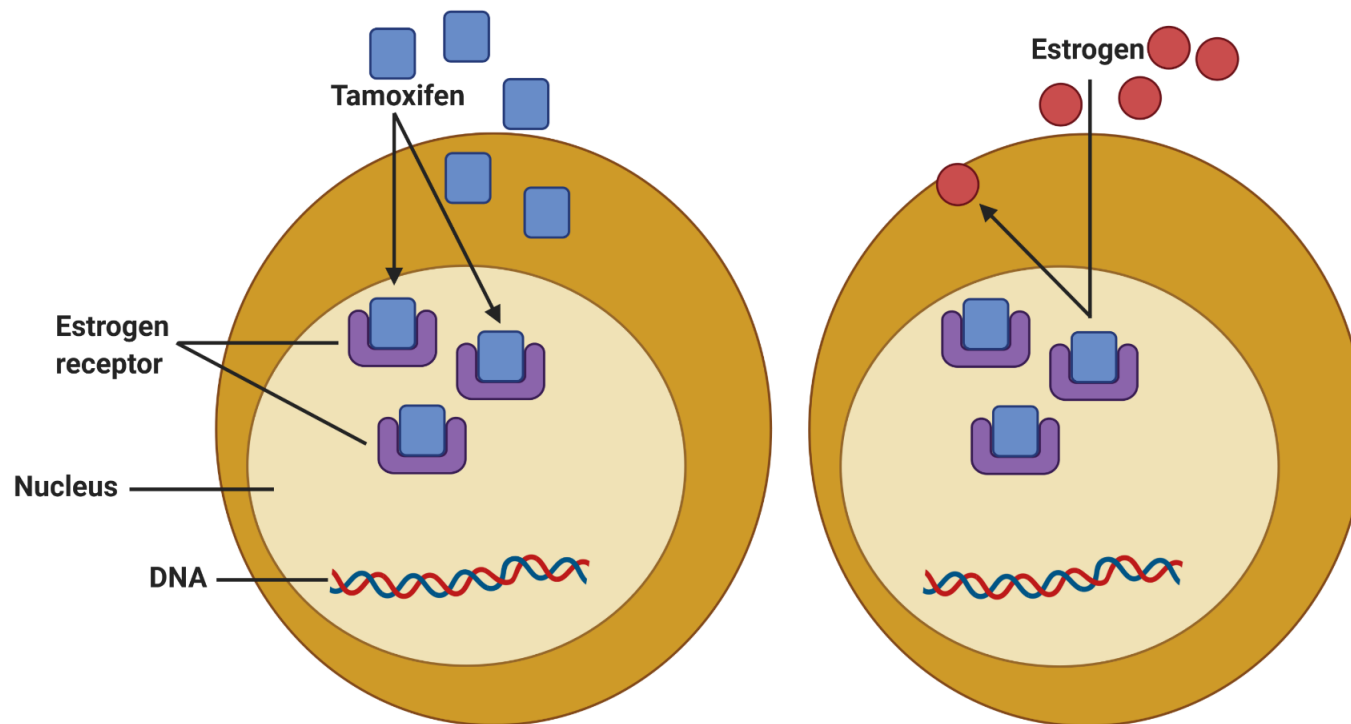


**Figure 1.3: Schematic diagram shows tamoxifen binding to oestrogen receptor and prevention of oestrogen to its receptor (adapted from <https://www.riverpharmacy.ca>). Created with BioRender.com.**

## 1.4 Chemoresistance

Resistance of cancer cell limits the effectiveness of chemotherapy. Cancer may be intrinsically drug-resistant or acquired-resistance to chemotherapy during course of treatment (Longley & Johnston, 2005; Holohan *et al.*, 2013; Clarke *et al.*, 2015). Intrinsic resistance is contributed by pre-existing intracellular resistance-mediating factors (Holohan *et al.*, 2013). In contrast, development of acquired drug resistance happens during treatment of tumours (Holohan *et al.*, 2013). Additionally, resistance can also be acquired through the selection pressure of a resistant population of cells. By such pressure it will cause the development of resistant cell population that has the ability to cause recurrence with larger evolvability characteristic (Foo & Michor, 2014; Sprouse & Herbert, 2014). Therefore, to reduce the incidence of breast cancer resistance, new therapy is needed to overcome this challenge.

In general, both pharmacokinetic factors and pharmacodynamic properties of the drugs have been associated with the development of drug resistance (Asaduzzaman, 2016). Cancer cells may use multiple mechanisms to escape drug treatment (Figure 1.4). This includes inadequate access of the drug to the tumour cells due to the inhibition of drug uptake (Asaduzzaman, 2016), or more commonly through increase of drug efflux (Sprouse, 2014). Proteins that are involved in drug efflux is controlled by the overexpression of multidrug efflux pumps such as P-glycoprotein (encoded by *MDR1*), MRP1 (encoded by *ABCC1*) and ABCG2 (encoded by *BCRP*) (Januchowski *et al.*, 2016; Spitzwieser *et al.*, 2016). Another mechanism to decrease the drug uptake is by compartmentalising the drug into intracellular vesicles, thus the drug would not be able to reach the target (Lu, 2015). Nevertheless, effect of the drug can be modulated by the capability of the cancer cell to repair DNA damage and enhance DNA repair mechanism (Zhu *et al.*, 2018). Deregulation of the cancer cell

cycle or ability to escape the apoptosis pathway enables the limitless cell division (Thu *et al.*, 2018). Recently, alteration of local drug metabolism (reprogrammed metabolism) (Hultsch *et al.*, 2018) and detoxification (Cree & Charlton, 2017) were reported as characteristics of cancer resistance.

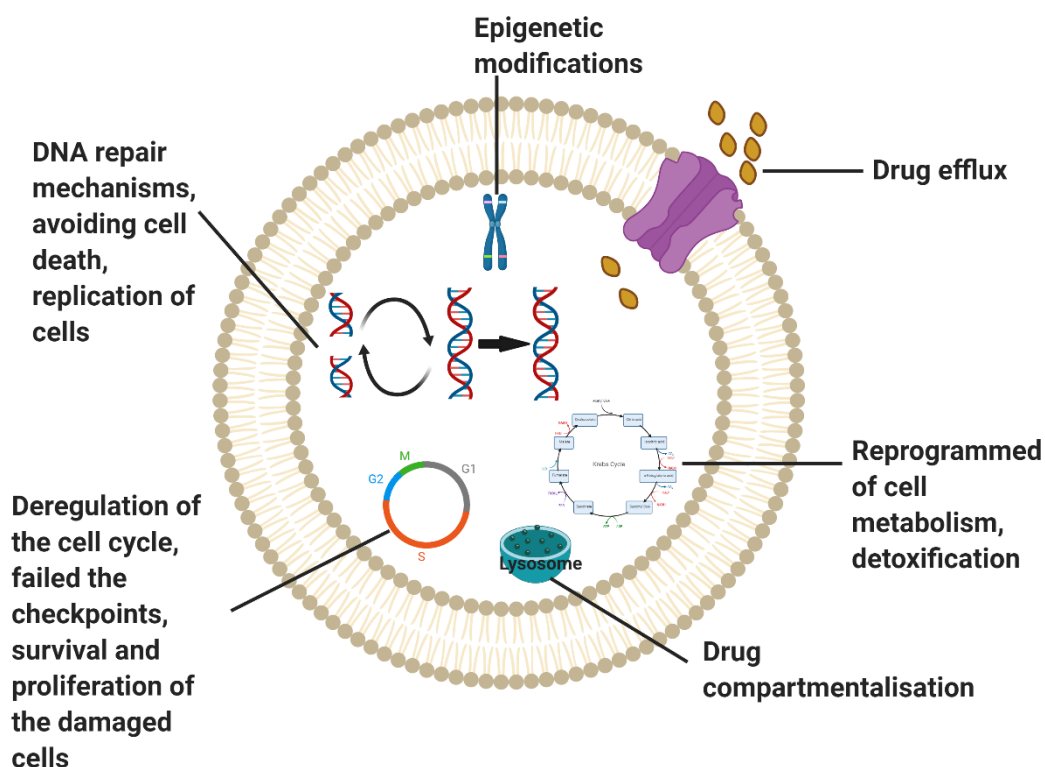


**Figure 1.4: Multiple mechanisms that are involved in the development of resistance to therapeutic agents. Created with BioRender.com.**

Although endocrine resistance is widely used, between 25-35% of the treated patients would develop recurrence. It can be contributed by either intrinsic or acquired resistance towards endocrine therapies (Haque & Desai, 2019). Potential mechanisms that have been associated with endocrine resistance involve alterations of cell survival and cell proliferation (Osborne & Schiff, 2011). Moreover, the acquisition of endocrine resistance is manifested by morphological changes that show epithelial-mesenchymal transition (EMT) transition along with increased migratory rate in both

anti-oestrogen resistant cells (Piggott *et al.*, 2018; Zhu *et al.*, 2018). Besides that, resistance to endocrine therapy is exhibited by tumour-inducing cells which is stem-like protrusions. This features could contribute to disease progression (Brien *et al.*, 2011; Luqmani & Alam-Eldin, 2016). Endocrine resistance exhibited higher expression of *cyclin-D1* gene that is involved in cell growth. Additionally it causes the activation of *CDK4* and *CDK6* genes in tandem with high expression of Bcl2 proteins, the anti-apoptotic protein (Rudas *et al.*, 2008). Endocrine resistance also modify the expression of proteins that are involve in cell cycle such as C-MYC, RB1, p21 and P27KIP1 (Thangavel *et al.*, 2011; Dixon, 2014). Besides cell cycle, the other mechanism involves ligand binding to growth receptors such EGFR, HER2 and IGF-1. Activation of the receptors would cause downstream signaling that involved NF- $\kappa$ B and PI3K/Akt/mTOR pathway.

This indicates that, resistant cells have the capability to survive even with existing mode of therapies. Therefore, to mitigate resistance to anti-cancer drug, there is a pressing need to explore into new drug as an alternative to the current therapies. Ongoing clinical trials are venturing new agents to be given along with endocrine therapy (Leary *et al.*, 2007; Alfakeeh & Brezden-Masley, 2018). Another possibility to overcome drug resistance is by materializing the herbal medicines that confer the anti-cancer properties. In addition, the plant-derived compounds have been the source of many chemotherapeutic agents (Mokashi, 2004; Wang *et al.*, 2015). Natural compounds like quercetin and curcumin have been used for treatment in clinical trials to overcome cancer drug resistance (Sotiropoulou *et al.*, 2014). Some studies have reported that alkaloids, flavonoids and other plant compounds could inhibit P-gp when given along with chemotherapeutic drugs (Lee *et al.*, 2018). One of the extensively studied plant is *Nigella sativa*, has long been regarded as the most treasured nutrient-

rich herbs in history around the world and numerous scientific studies are in progress to validate the traditionally claimed uses of small seed of this species (Mariod *et al.*, 2017; Ahmad *et al.*, 2019).

### 1.5 *Nigella sativa*

*Nigella sativa* L. (*N. sativa*) is a small shrub (20-90 cm tall) from the family *Ranunculaceae*. It is native plant to Southern Europe, North Africa and Southeast Asia. *N. sativa* has tapering green leaves and rosaceous white, yellow, pink, pale blue or purplish flowers with 5-10 petals. The ripe fruit (capsule: 3-7 united follicles) contains numerous tiny seeds, dark black in color and possess a severe pungent smell, contains considerable amount of oil (Figure 1.5). *N. sativa* was first botanically described and characterized by Linnaeus in 1753 (Table 1.2).

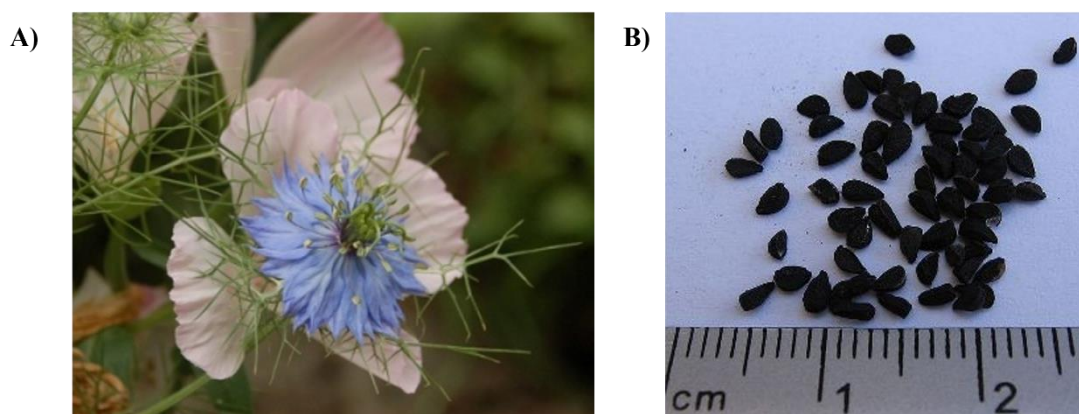


**Figure 1.5:** *Nigella sativa* flower (A) and black seeds (B). (Adapted from <http://bioweb.uwlax.edu/bio203/>)

**Table 1.2: Taxonomic group of *Nigella sativa* (NCBI: txid555479)**

<b>Kingdom</b>	<b>Plantae</b>
Order	Ranunculales
Family	Ranunculaceae
Genus	<i>Nigella</i>
Species	<i>N. sativa</i>

The black seeds of *N. sativa* (Ranunculaceae) have been mentioned in many historical and religious references. The black seed contains several components of the volatile oil including TQ (2-Isopropyl-5-methylbenzo- 1,4-quinone, 30-48%), thymohydroquinone, dithymoquinone, p-cymene (7-15%), carvacrol (6-12%), 4-terpineol (2-7%), t-anethol (1-4%), sesquiterpene longifolene (1-8%),  $\alpha$ -pinene and thymol (Ali & Blunden, 2003; Islam, 2018). TQ has been reported to exhibit anti-oxidant (Dur *et al.*, 2016; Imran *et al.*, 2018), anti-inflammatory (Woo *et al.*, 2013; Ballout *et al.*, 2018) and chemo-sensitization effects (Mostofa *et al.*, 2017). The antiproliferative effects of TQ have been reviewed by Almajali *et al.* (2021) in many types of cancer, such as breast cancer, lung cancer, gastric cancer, colon cancer, prostate cancer, skin cancer, ovarian cancer, liver, cervical cancer and blood cancer. Additionally, TQ protects healthy cells from oxidative damage, making it an efficient chemotherapeutic agent (Ecevit *et al.*, 2017; Mariod *et al.*, 2017).

## **1.6 Thymoquinone: A Promising Drug for Circumventing Multidrug Resistance (MDR)**

TQ, discovered as a substantial component of the volatile oil (hydrophobic chemical compounds from plants that can easily evaporate at normal temperatures), is the most bioactive chemical and demonstrates a wide range of therapeutic advantages among the several active ingredients reported thus far (Mariod *et al.*, 2017). TQ shows

potential pharmacological properties such as anti-oxidant, anti-inflammatory, anti-cancer and other important biological activities (Khan *et al.*, 2011). These pharmacological effects of TQ are due to quinone constituent (Figure 1.6). It inhibited cancer cell growth and progression based on *in vitro* and *in vivo* study models (Majdalawieh *et al.*, 2017; Ballout *et al.*, 2018). Moreover, TQ has also been found to be cytotoxic in several types of parental and multi-drug resistant human tumour cell lines (<https://patents.justia.com/patent/6218434>, Worthen *et al.*, 1998; Ali & Blunden, 2003).

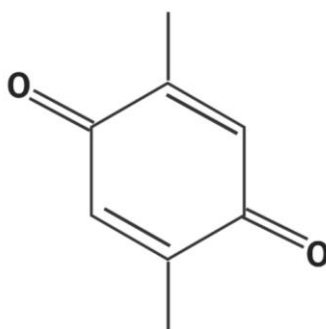


**Figure 1.6: Chemical structure of TQ. PubChem SID=386221103. (<https://pubchem.ncbi.nlm.nih.gov/substance/386221103>). Created with BioRender.com**

For instance, TQ treatment showed promising results in doxorubicin-resistant human breast cancer cells (Arafa *et al.*, 2011). There was an extensive decrease of the cell survival regulators, phosphorylated Akt and Bcl2 along with an increased expression of PTEN and apoptotic markers such as Bax, cleaved caspases, and cleaved PARP after doxorubicin-resistant MCF-7/DOX cells were exposed to TQ. TQ also produced an augmented expression of p53 and p21 proteins with a concomitant G2/M arrest in the same cell line.

Meanwhile, study by Bashmail *et al.* (2018) had assessed the chemomodulatory potential of TQ to gemcitabine (GCB) against human breast

adenocarcinoma (MCF-7) and ductal carcinoma (T47D) cells. TQ induced apoptosis, necrosis, and autophagy in MCF-7 and T47D breast cancer cells, demonstrating cytotoxic effects and promising chemo-modulatory effects to GCB against these breast cancer cells, in addition to depleting tumour associated resistant stem cell fraction (Bashmail *et al.*, 2018). Although the use of GCB was clinically approved for the treatment of metastatic breast cancer since 2004, it suffers from many drawbacks such as lack of selectivity, exaggerated normal tissue toxicity and the emergence of tumour resistance (Barton-Burke, 1999; Burstein, 2000) and appear in the form of tumour relapse and/or recurrence and remote organ metastasis (Jia & Xie, 2015). Therefore, TQ might be able to overcome resistance to GCB and would be a potential successful therapy for breast cancer.

A separate study have demonstrated anti-proliferative and pro-apoptotic activities of TQ in both a non-small cell lung cancer (NSCLC) and a small cell lung cancer SCLC cell lines (Jafri *et al.*, 2010). It also appears that there may be synergism between TQ and cisplatin. This combination was active *in vivo* as demonstrated by the mouse xenograft study. By suppressing NF- $\kappa$ B, TQ may be able to overcome ciplastin resistance and enhance its efficacy. Thus, TQ or likely synthetic analogues of TQ should be developed for possible future human use not only in lung cancer but in possibly other tumour types as well.

TQ anti-cancer activities have been studied in numerous experimental animal models (Khan *et al.*, 2011; Goyal *et al.*, 2017). Although it has been extensively studied, its application in clinical setting is still limited due to its poor bioavailability and hydrophobicity (Odeh *et al.*, 2012; Ballout *et al.*, 2018) for considering it as the primary therapeutic agent. In order to overcome TQ solubility and biodistribution, TQ

encapsulation may improve its delivery to the target sites (Ballout *et al.*, 2018) (Figure 1.7)

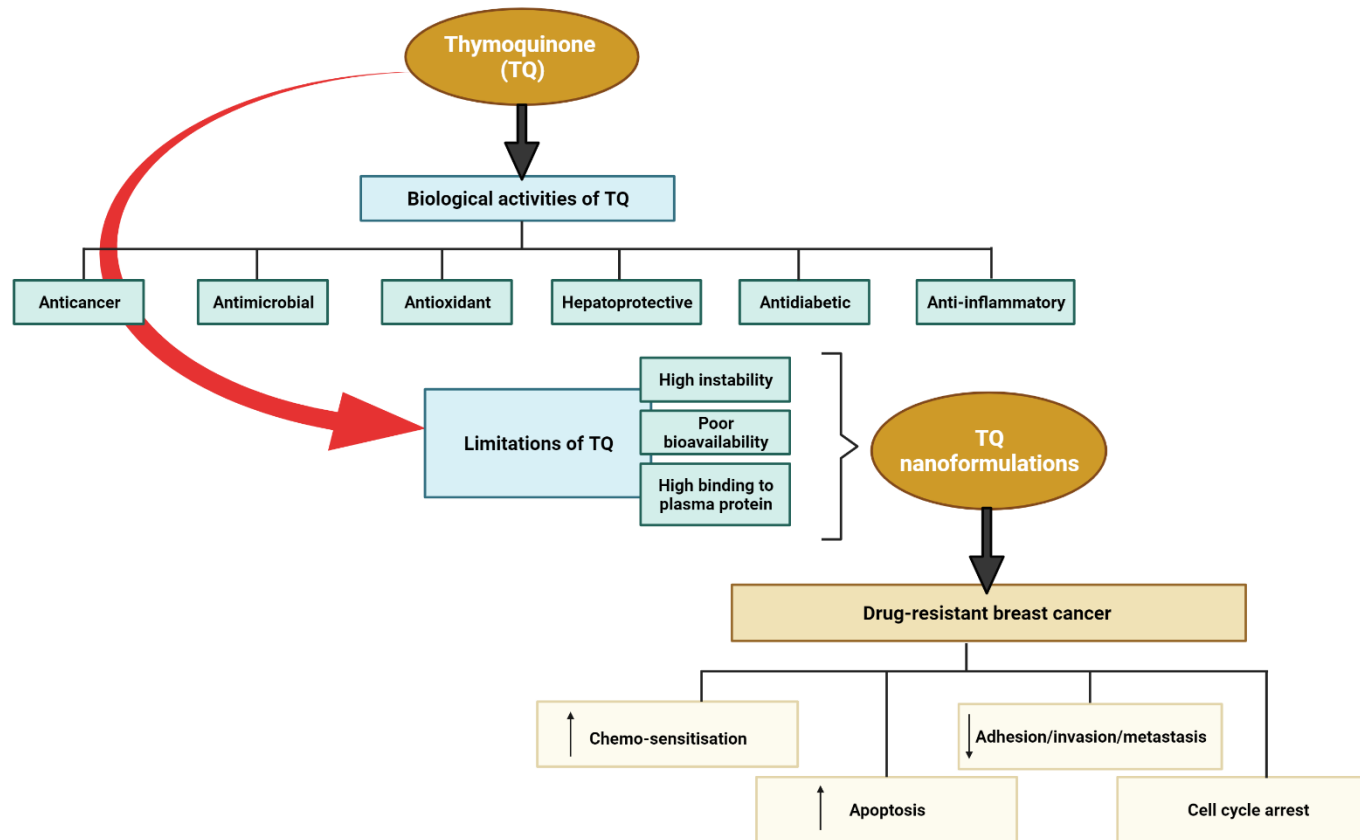


Figure 1.7: Multitargeted protective effects of TQ mechanism against drug-resistant breast cancer. Created with BioRender.com.

## 1.7 Nanoparticulates to Treat Breast Cancer

Nanoparticulates have been gaining research interest over the recent years. Their application in cancer therapy has given promising findings over existing breast cancer therapy that includes surgery, radiotherapy, chemotherapy and hormonal therapy (Hortobagyi, 1998). These therapies demonstrate low specificity and side effects towards the patients (Adair *et al.*, 2010; Tang *et al.*, 2017). For instance, doxorubicin from the family of anthracyclines promotes cardiotoxicity in patients with breast cancer (Smith *et al.*, 2010). This is due to the fact that their ability to treat cancer is hampered by cumulative dose-dependent cardiotoxicity, which can result in irreparable heart failure (Volkova & Russell, 2012; Cai *et al.*, 2019). Studies in cells and animals reveal that the mechanism of anthracycline-induced cardiotoxicity (AIC) is multifaceted, with free radical generation inducing numerous types of cellular harm (Geisberg & Sawyer, 2010; Cai *et al.*, 2019). In addition, anthracyclines alter nucleic acid biology by intercalation into DNA and modulate intracellular signaling, leading to cell death and the disruption of homeostatic processes such as sarcomere maintenance (Rawat *et al.*, 2021). Meanwhile, paclitaxel and docetaxel from the family of taxanes caused bone marrow suppression (Nurgalieva *et al.*, 2011) and hypersensitivity reactions (Lee *et al.*, 2009) in the breast cancer patients. Compared with conventional cancer therapies, nanomedicine has many benefits, as they are less prone to drug degradation while being transported. The other advantage includes improve biocompatibility and increase delivery of drug to tissues. The ideal characteristics of a nanoparticle should comprise various aspects such as non-toxic, biocompatible, nano-scale size, encapsulation efficiency, stability, drug release and targeting sites (Table 1.3). Nanomedicine also exhibits great potential to effectively target and eliminate breast cancer stem cells, which are involved in resistance. List of

formulations for breast cancer therapeutics with approval of Food and Drug Administration (FDA) and ongoing clinical trials are provided in Table 1.4. The liposomes, polymeric nanoparticles and nanoparticle albumin-bound (Nab™)-paclitaxel are the most common nanoparticles designed to treat breast cancer (Figure 1.8).

**Table 1.3: Selection criteria for a nanoparticulate-based therapeutic platform.**

Desired characteristics	Comments
Inherently nontoxic and biocompatible materials	The initial material selections should be based on nontoxic and biocompatible materials especially with an aim toward human healthcare.
Small size (10-200 nm)	This is a proven range of effective particle diameter for a wide variety of delivery system. However, there is no particular size that seems most efficacious, especially for <i>in vivo</i> studies.
Encapsulation of active agent	The active agents/drugs must be encapsulated within the nanoparticles to be protected from unwanted degradation or clearance during blood circulation. To achieve the therapeutic dosage, the nanoparticles must encapsulate a high percentage of the active agents/drugs (>50%).
Colloidally stable in physiological conditions/environments	The nanoparticles and surface functionalisation should be resistant to agglomeration caused by solution Ph values, ionic strength, macromolecular interactions, and temperature encountered in the physiological environment.
Targeting to cell or tissue of choice	Targeting ensures the greatest uptake concentration of chemotherapeutics within the desired lesions and the least side effects with healthy tissues.
Biologically or extrinsically controlled release of active agents	There should be a trigger mechanism such as the acidic Ph within the tumour or during endosome maturation to

	ensure the release of the encapsulated drug into the targeted tissues
Reasonable circulation time	<p>Resistance to agglomeration that remove the nanoparticle-encapsulated drug from the patient must be avoided to promote long circulation times in the circulatory system for as many of the nanoparticles to find and sequester in the cancer cells as possible.</p> <p>There must be clearance mechanisms for the nanoparticle vehicle after completing its task, to avoid the cumulative and/or systemic side effects such as interference with biological functions.</p>

Adapted with permission from Adair *et al.* (2010).

**Table 1.4: List of nanomedicines as breast cancer therapeutics approved by the U.S. FDA and those in clinical trials.**

<b>Product</b>	<b>Nanoplatfrom/agent</b>	<b>Manufacturer (in USA)</b>	<b>Status in USA</b>	<b>Reference/Clinical trial identifier</b>
Doxil®	PEGylated liposomal/doxorubicin hydrochloride	Janssen Products	Approved in 1995	Barenholz, 2012
Abraxane®	Nanoparticle albumin-bound paclitaxel	Abraxis Bioscience	Approved in 2005	Hawkins <i>et al.</i> , 2008
Myocet®	Non-PEGylated liposomal/doxorubicin	Sopherion Therapeutics	Phase III	NCT00294996
NK-105	PEG-polyaspartate/paclitaxel	Nippon Kayaku	Phase III	NCT01644890
Genexol® -PM	PEG-poly (D, L-lactide)/paclitaxel	Samyang Biopharmaceuticals	Phase III	NCT00876486
NK-012	PEG-polyglutamic acid/SN-38	Nippon Kayaku	Phase II	NCT00951054
Xyotax®	Paclitaxel poliglumex	Dana-Farber Cancer Institute	Phase II	NCT00148707
ThermoDox®	Heat-activated liposomal/doxorubicin	Celsion	Phase I/II	NCT00826085
Liposomal annamycin	Liposome/semi-synthetic doxorubicin analogue annamycin	New York University, School of Medicine	Phase I/II	NCT00012129

Rexin-G	Targeting protein tagged phospholipid/microRNA-122	Epeius Biotechnologies	Phase I/II	NCT00505271
SPI-077	Stealth liposomal cisplatin	LiPlasome Pharma	Phase I	NCT01861496
S-CKD602	PEGylated liposomal/CKD602	Alza	Phase I	NCT00177281
Nanoxel®	PEG-poly (D, L-lactide)/docetaxel PEG-Polylactic-co-glycolic	Fresenius Kabi Oncology	Phase I	NCT00915369
BIND-014	PEG-Polylactic-co-glycolic acid/docetaxel	BIND	Phase I	NCT01300533

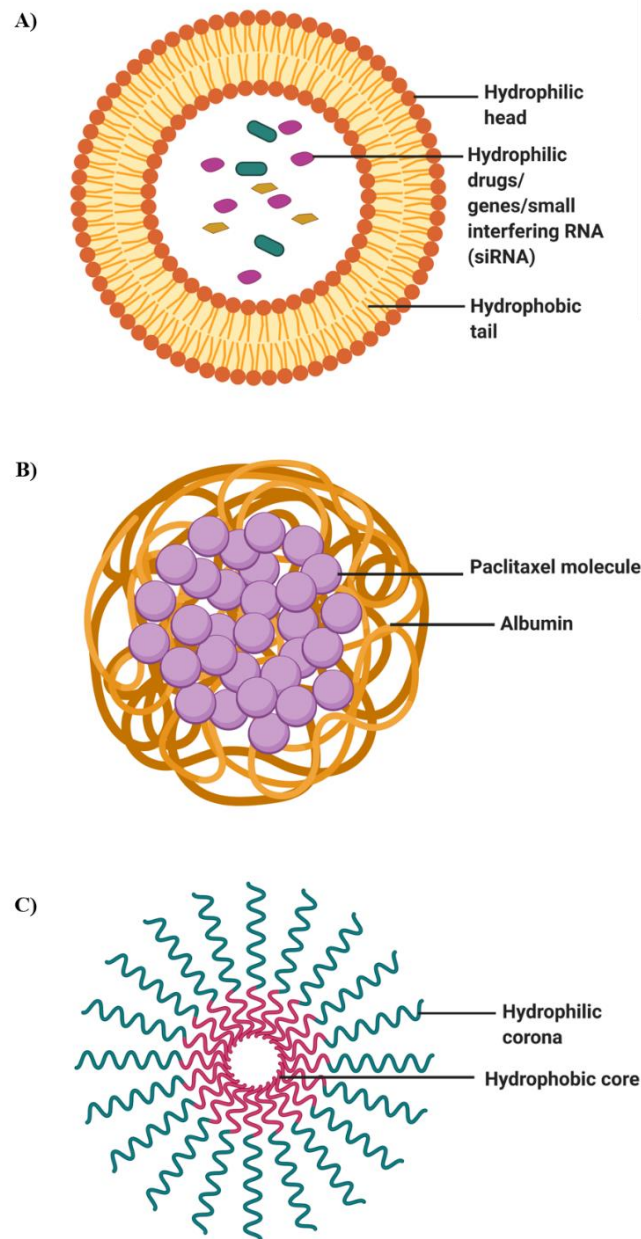


**Figure 1.8: Nanoparticulate-based chemotherapeutic delivery platforms approved by the US FDA for cancer treatment. (A) Liposomes are spherical vesicle composed of an aqueous core and a membranous lipid bilayer, preferable for encapsulation of hydrophilic drugs; (B) Nanoparticle albumin-bound paclitaxel (Nab-paclitaxel) is a colloid suspension of paclitaxel; (C) Polymeric nanoparticles are self-assembled from amphiphilic and biodegradable polymers in aqueous solution and are effective to encapsulate hydrophobic drugs. Created with BioRender.com.**